



**HAL**  
open science

# Serotype-specific Binding Properties and Nanoparticle Characteristics Contribute to the Immunogenicity of rAAV1 Vectors

Maxime Ferrand, Sylvie da Rocha, Guillaume Corre, Anne Galy, Florence Boiségerault

► **To cite this version:**

Maxime Ferrand, Sylvie da Rocha, Guillaume Corre, Anne Galy, Florence Boiségerault. Serotype-specific Binding Properties and Nanoparticle Characteristics Contribute to the Immunogenicity of rAAV1 Vectors. *Molecular Therapy*, 2015, 23 (6), pp.1022-1033. 10.1038/mt.2015.59 . hal-02178340

**HAL Id: hal-02178340**

**<https://univ-evry.hal.science/hal-02178340>**

Submitted on 5 Dec 2023

**HAL** is a multi-disciplinary open access archive for the deposit and dissemination of scientific research documents, whether they are published or not. The documents may come from teaching and research institutions in France or abroad, or from public or private research centers.

L'archive ouverte pluridisciplinaire **HAL**, est destinée au dépôt et à la diffusion de documents scientifiques de niveau recherche, publiés ou non, émanant des établissements d'enseignement et de recherche français ou étrangers, des laboratoires publics ou privés.

# Serotype-specific Binding Properties and Nanoparticle Characteristics Contribute to the Immunogenicity of rAAV1 Vectors

Maxime Ferrand<sup>1,2</sup>, Sylvie Da Rocha<sup>1,2</sup>, Guillaume Corre<sup>1,2</sup>, Anne Galy<sup>1,2</sup> and Florence Boisgerault<sup>1,2</sup>

<sup>1</sup>Inserm, U951, "Integrare" research unit, R&D department, Genethon, Evry, F91002 France; <sup>2</sup>University of Evry, UMR\_S951, Evry, F91002 France

The immunogenic properties of recombinant adeno-associated virus (rAAV) gene transfer vectors remain incompletely characterized in spite of their usage as gene therapy vectors or as vaccines. Molecular interactions between rAAV and various types of antigen-presenting cells (APCs), as well as the impact of these interactions on transgene or capsid-specific immunization remain unclear. We herein show that binding motifs recognized by the capsid and which determine the vector tissue tropism are also critical for key immune activation processes. Using rAAV capsid serotype 1 (rAAV1) vectors which primary receptors on target cells are  $\alpha 2,3$  and  $\alpha 2,6$  N-linked sialic acids, we show that sialic acid-dependent binding of rAAV1 on APCs is essential to trigger CD4<sup>+</sup> T-cell responses by increasing rAAV1 uptake and contributing to antigenic presentation of both the capsid and transgene product although this involves different APCs. In addition, the nanoparticulate structure of the vector in itself appears to be sufficient to trigger mobilization and activation of some APCs. Therefore, combinations of structural and of serotype-specific cell-targeting properties of rAAV1 determine its complex immunogenicity. These findings may be useful to guide a selection of rAAV variants depending on the intended level of immunogenicity for either gene therapy or vaccination applications.

Received 21 October 2014; accepted 10 March 2015; advance online publication 5 May 2015. doi:10.1038/mt.2015.59

## INTRODUCTION

Recombinant adeno-associated virus (rAAV) vectors are small viral nanoparticles (~26 nm) constituted of a viral icosahedral protein capsid surrounding a single-stranded DNA gene expression cassette with an estimated isoelectric point of about 6–6.6.<sup>1,2</sup> While several applications of rAAV as genetic vaccines have been reported,<sup>3,4</sup> these viral vectors are also commonly used for gene transfer applications in genetic diseases, based on their ability to safely transduce post-mitotic tissues with relatively low immunogenicity as compared to other vectors like recombinant adenoviruses. However, deleterious anti-capsid and anti-transgene cellular immune responses have been observed following rAAV-mediated

gene transfer in animal models and in human trials<sup>5,6</sup> while at the same time evidence of tolerance against the vector capsid or transgene has also been reported,<sup>7–9</sup> raising important questions about the nature of rAAV determinants involved in its immunogenicity.

A wide variety of nanoparticles have been used as DNA or protein delivery systems for vaccination approaches, with the objective of targeting and stimulating antigen-presenting cells (APC) to induce protective immune responses (for review<sup>10</sup>). By mimicking a native viral structure, virus-like particles can often strongly stimulate innate and adaptive immune responses and become potent vaccines. Nanoparticle-based vaccines can exploit various physical and chemical properties that influence the targeting, processing of the antigens and signals delivered to dendritic cells (DC), a highly specialized population of APC able to prime T cells<sup>11,12</sup>). Several subtypes of DCs exist with specialized pathogen sensors and immune-activating properties (reviewed recently<sup>13,14</sup>). Pathogen-associated molecular patterns for pattern recognition receptors such as toll-like receptors (TLR) and C-type lectin receptors, but also damage-associated molecular patterns play crucial role in DC activation. The activation status of DCs determines the orientation of CD4<sup>+</sup> T cells toward either a tolerogenic or "helper" phenotype.<sup>15</sup> With regard to T-cell activation, if conventional or classical CD11c<sup>+</sup> DC (cDC) are often essential players, there is also increasing evidence that plasmacytoid DC (pDC), B cells and macrophages have additional roles.<sup>16–18</sup> In mice, rAAV-mediated gene transfer *in vivo* leads to the transduction of DCs<sup>19</sup> and to the presentation of the transgene product to T cells with induction of T-cell responses.<sup>20</sup> The properties of rAAV leading to its immunogenicity are not fully understood but known to be influenced by intrinsic characteristics such as the capsid serotype and the structure of the encapsidated DNA.<sup>21,22</sup> To explore what other determinants are involved in the immunogenicity of rAAV gene transfer, we focused on vectors engineered with capsid serotype 1 (rAAV1) which are capable of inducing T-cell and antibody responses in mice against both the vector capsid and the transgene.<sup>20,23,24</sup> In particular, we have shown the importance of MHC class II presentation to CD4 T cells for the production of neutralizing antibodies against the rAAV1 capsid<sup>24</sup> and for effector T-cell-mediated rejection and the production of antibodies against the transgene.<sup>20,23</sup> In this model, CD11c<sup>+</sup> cDC efficiently processed and presented transgene-derived T-cell epitopes *in vivo* following intramuscular (IM) delivery.<sup>20</sup> However, it is not known

Correspondence: Florence Boisgerault, Genethon, UMR951, 1 bis rue de l'Internationale 91002 Evry, France. E-mail: fboisgerault@genethon.fr Or Anne Galy, Genethon, UMR951, 1 bis rue de l'Internationale 91002 Evry, France. E-mail: galy@genethon.fr

if other APCs contribute to the antigenic presentation of this vector or of the transgene in case of systemic administration and what properties of the vector and APCs are involved.

The primary receptors of rAAV1 are known to be  $\alpha 2,3$  and  $\alpha 2,6$  N-linked sialic acids<sup>25</sup> which are known to be expressed on many types of cells including APCs.<sup>26</sup> Many viruses use sialylated glycans for attachment and entry<sup>27</sup> and sialylated receptors are involved in many cell adhesion functions particularly in the immune system and for APC functions such as phagocytosis, endocytosis, migration, and the capacity to induce T-cell responses.<sup>26</sup> Therefore, the engagement of sialic acids on APC by rAAV1 may play a role in T-cell immunity and involve different mechanisms. In addition, the pattern and the density of sialic acid modifications differ with regard to the origin, differentiation, and the maturation of APC,<sup>28</sup> possibly orienting the vector tropism toward specific subpopulations of APC and affecting its immunogenicity, but this has not yet been examined functionally. Here, we showed in mice that sialic acid-dependent interactions of rAAV1 with DC and macrophages contribute in a different manner to the establishment of anti-capsid and anti-transgene-specific CD4<sup>+</sup> T-cell responses. In addition, the nanoparticulate nature of the vector also contributes to the overall activation and recruitment of those APC. Thus, both structure and specific receptors determine the complex immunogenicity of rAAV1.

## RESULTS

### Capsid immunogenicity is determined by sialic acid-dependent interactions with CD11c<sup>+</sup> DC and CD11b<sup>+</sup> cells

Various types of APCs contribute to T-cell responses and CD11c<sup>+</sup> DC are endowed with the unique capacity to prime naive T cells. The critical importance of CD11c<sup>+</sup> DC for capsid immunization was verified in a conditional *in vivo* depletion model which is based on the transplantation into normal mice, of bone marrow from CD11c-DTR transgenic mice.<sup>29</sup> In this protocol, 90% donor chimerism was achieved in the blood of recipient mice, which recovered normal blood counts 8–9 weeks after transplantation (Table 1). Such chimeric mice were capable of mounting robust anti-AAV1 capsid T-cell responses following the administration of a capsid-tagged vector (rAAV1-DBY). The tagged capsid induces the same level of anti-capsid antibodies as the nontagged AAV1 capsid but it contains the MHC class II Dby peptide of the HY male antigen inserted in position 34 of VP1, providing an easily detectable CD4<sup>+</sup> T-cell epitope to measure capsid antigenic presentation and capsid-specific CD4<sup>+</sup> T-cell responses as previously reported.<sup>24</sup> The administration of diphtheria toxin (DT) to kill DTR<sup>+</sup> cells

in these chimeric mice depleted about 80% of all CD11c<sup>+</sup> DC in spleen and lymph nodes as measured 1 day after the last injection of DT (Table 2). In such DC-depleted mice, the injection of a rAAV1-DBY showed a 50% reduced anti-capsid CD4<sup>+</sup> T-cell response compared to mock-treated animals (Figure 1a). These results establish that CD11c<sup>+</sup> DC play a major role in the initiation of CD4<sup>+</sup> T-cell immune responses against the vector capsid *in vivo*. To demonstrate the direct involvement of CD11c<sup>+</sup> DC in antigenic presentation and to assess the contribution of other APCs such as CD11b<sup>+</sup> macrophages and CD19<sup>+</sup> B cells in this process, we compared the ability of these different populations of APCs to present capsid epitopes to T cells after systemic administration of the vector in normal mice. These various populations of APC were purified from the spleens of mice injected intravenously (IV) with rAAV1-DBY. Antigenic presentation capacity was evaluated *ex vivo* by coculturing the purified APCs with Dby-specific T cells and detecting T-cell division. In this system, antigenic presentation of the capsid was only promoted by CD11c<sup>+</sup> DC but neither by CD11b<sup>+</sup> macrophages nor by CD19<sup>+</sup> B cells (Figure 1b). Yet all three of these populations of APC had the intrinsic ability to present the Dby peptide to specific CD4<sup>+</sup> T cells *in vitro* (Supplementary Figure S1a). Thus, CD11b<sup>+</sup> macrophages and B cells display sufficient numbers of MHC II molecules to present to CD4<sup>+</sup> T cells but do not contribute in a major way to antigenic presentation of the rAAV1 capsid *in vivo*. Similar findings were made following IM injections of rAAV1-DBY and show that in the spleen or in lymph nodes, the capsid is essentially presented by CD11c<sup>+</sup> DC (Supplementary Figure S1b).

The overall contribution of sialic acids to this antigenic presentation process was first evaluated *in vitro*, then *in vivo* using neuraminidase (NA) to remove sialic acids on the surface of various cells. *In vitro*, NA-treated splenic CD11c<sup>+</sup> DC and

**Table 2 Depletion of CD11c<sup>+</sup> cells after DT treatment**

a)	%CD11c <sup>+</sup>	%CD11b <sup>+</sup>	%CD3 <sup>+</sup>	%CD19 <sup>+</sup>
PBS	0.875 ± 0.06	5.50 ± 0.06	24.94 ± 5.0	69.3 ± 4.96
DT	0.093 ± 0.05	6.55 ± 0.86	21.10 ± 2.3	72.6 ± 2.63
b)	%CD11c <sup>+</sup>	%CD11b <sup>+</sup>	%CD3 <sup>+</sup>	
PBS	0.12 ± 0.09	1.75 ± 1.15	29.1 ± 2.59	
DT	0.02 ± 0.02	1.73 ± 0.82	21.5 ± 3.51	

Analysis of cell populations in **a)** spleen or **b)** draining lymph nodes following injection of DT or PBS in mice. Results are expressed as the mean ± SD of the percentage of CD11c<sup>+</sup>, CD11b<sup>+</sup>, CD3<sup>+</sup> or CD19<sup>+</sup> cells measured by FACS among live cells from 6 independent experiments with 3 mice per group. FACS, fluorescence activated cell sorting.

**Table 1 Hematological reconstitution of chimeric CD11c-DTR mice after transplantation**

Blood analysis	White blood cell counts × 10 <sup>9</sup> /l			(Blood) platelet counts × 10 <sup>9</sup> /l
	%Lymphocyte	%Monocyte	%Granulocyte	
Grafted	12.05 ± 2.84	87.7 ± 3.05	6.48 ± 1.3	916 ± 313
Control	14.10 ± 2.77	85.0 ± 2.59	8.40 ± 0.8	1,441 ± 337
Spleen analysis	%CD45.1 <sup>+</sup>	%CD45.2 <sup>+</sup>		
Grafted	11.34 ± 2.35	88 ± 2.37		
Control	100 ± 0.05	0 ± 0		

Hematological reconstitution in blood and donor chimerism in spleen observed 8–9 weeks after transplantation of CD11c-DTR bone marrow in six independent experiments with 20 mice per experiment. Controls are age-matched C57Bl/6 mice nonirradiated and nontransplanted. Results are expressed as mean values ± SD.

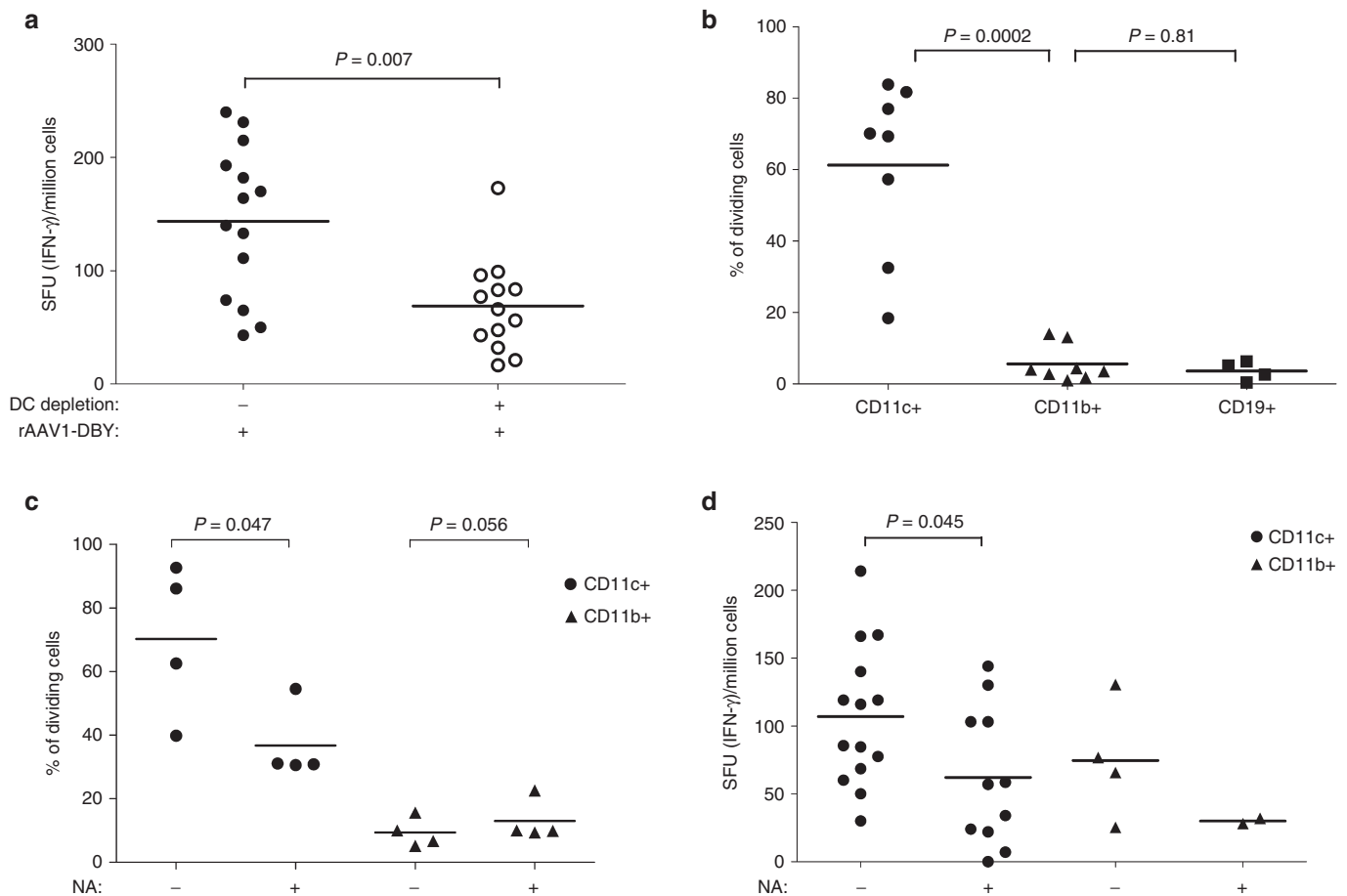


**Figure 1** Antigenic presentation and functional contribution of sialic acids on DC for rAAV1 capsid immunogenicity. **(a)** The role of CD11c+ cells in the anti-capsid CD4<sup>+</sup> T-cell response was investigated by injecting the rAAV1-DBY vector ( $5.10^9$  vg/mice, IM) to mice depleted (+) or not (-) of CD11c+ cells and measuring the IFN- $\gamma$  response in the spleen after 8 days. Prior to the injection of vector, mice were transplanted with CD11c-DTR bone marrow and CD11c+ cells were depleted in the chimeric animals by three repeated DT injections. Data represent four experiments, each including at least three mice per group. Dots represent individual mouse data and horizontal bars indicate the average value. **(b)** Antigenic presentation of capsid by different populations of APCs was tested *ex vivo* following IV injection of the rAAV1-DBY vector to C57BL/6 mice. Purified CD11c+ (circle), CD11b+ (triangle), CD19+ (square) cells were prepared from the spleens of vector-injected mice and were cultured *ex vivo* with Dby-specific and CFSE-stained CD4<sup>+</sup> T cells from Marylin mice at different ratios. The graph represents results obtained with ratios of 1 APC to  $10^5$  T cells. Antigenic presentation was evident from the induced CD4 T-cell division measured by FACS as illustrated in **Supplementary Figure S1a** and results are expressed as % of cells having undergone at least one cell division. Data represent between five and eight experiments. Each dot represents the average antigen presentation value obtained in one experiment on a specific cell type using three mice. Horizontal bars indicate the average value of all experiments per cell type. **(c)** The functional contribution of sialic acid on *in vitro* antigenic presentation of the rAAV1 capsid was measured by incubating NA-treated (+) or nontreated (-) CD11c+ (circles) or CD11b+ (triangles) cells with the rAAV1-DBY vector for 1 hour then washing cells and incubating them with Dby-specific and CFSE-stained CD4<sup>+</sup> T cells from Marylin mice to measure antigenic presentation by FACS as detailed above. Data are representative of four experiments with four mice per group. **(d)** The importance of sialic acids on APCs was measured *in vivo*. CD11c+ (circles) or CD11b+ (triangles) cells that were previously NA-treated (+) or not (-) were incubated with rAAV1-DBY and were injected to C57BL/6 mice ( $10^6$  cells IV). After 8 days, IFN- $\gamma$  CD4<sup>+</sup> T-cell responses were measured in the spleen by enzyme-linked immunospot assays. Each dot represents one mouse and two to five experiments are shown. Some points had to be discarded due to enzyme-linked immunospot assays signal saturation. Statistical analysis was used to compare the effect of NA on CD11c+ cells in five experiments. FACS, fluorescence activated cell sorting.

CD11b+ macrophages were incubated with the rAAV1-DBY vector and subsequently cocultured with specific CD4<sup>+</sup> T cells. Removal of sialic acids on CD11c+ DC significantly decreased the antigenic presentation of the capsid compared to controls without NA digestion (**Figure 1c**). CD11b+ cells remained inefficient at presenting capsid antigens *in vitro*, regardless of NA treatment. To evaluate *in vivo* the contribution of sialic acids on antigenic presentation, mice were injected with rAAV1-loaded CD11c+ DC or CD11b+ macrophages that were treated or not with NA. These experiments confirmed that CD11c+ DC had the strongest capacity to present the capsid *in vivo* and required

sialic acids to induce an optimal anti-capsid CD4<sup>+</sup> T-cell response (**Figure 1d**). Unexpectedly, the injection of rAAV1-loaded CD11b+ also induced sialic-acid-dependent CD4 T-cell responses in this model although this was lower than CD11c+ cells. Possibly, CD11b+ cells indirectly provide antigens to cDC as these cells are not able to directly present the capsid to T cells *in vitro* (**Figure 1c**). Altogether, those data show that capsid antigenic presentation to T cells is essentially performed by CD11c+ DC and is mediated by the presence of sialic acids on these cells. Sialic acids on macrophages may indirectly help to provide antigen *in vivo*.

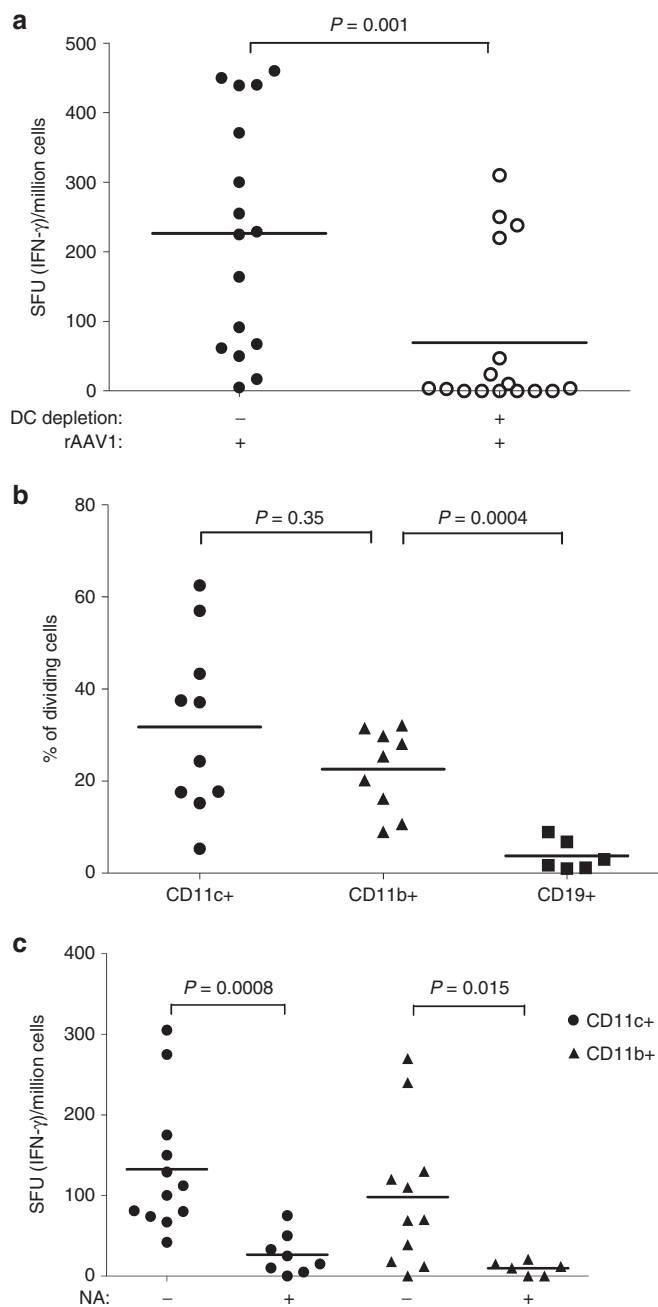


**Figure 2** Involvement of sialic acids on DC and macrophages for anti-transgene immune responses. **(a)** The role of CD11c+ cells in the anti-transgene immune response was investigated by IFN- $\gamma$  enzyme-linked immunospot assays 14 days after the IM administration of rAAV1-SGCA\_HY vector ( $5.10^9$  vg/mice) to chimeric CD11c\_DTR mice depleted (+) or not (-) of DC as described in Figure 1a. Data represent four experiments, each including three mice per group. **(b)** The *ex vivo* antigenic presentation of the transgene to CD4<sup>+</sup> T cells by CD11c+ (circle), CD11b+ (triangle), CD19+ (square) cells was measured following IV injection of rAAV1-SGCA\_HY and was evaluated by FACS as in Figure 1b. Data are representative of seven experiments. **(c)** Anti-transgene immune response was evaluated by IFN- $\gamma$  enzyme-linked immunospot assays in C57BL/6 mice injected IV with  $10^6$  CD11c+ or CD11b+ cells previously treated (+) or not (-) with NA and loaded with rAAV1-SGCA\_HY. Data are representative of three experiments with four mice per group. Dots represent individual mouse data and horizontal bars indicate the average value. FACS, fluorescence activated cell sorting.

### Sialic acids on DC and macrophages are involved in the anti-transgene immune responses

To examine T-cell responses against the transgene product, we again used a T-cell epitope-tagging strategy. Here, rAAV1 with a native capsid is used to deliver a transgene encoding an  $\alpha$ -sarcoglycan protein fused to the Dby peptide (Sgca-HY) as previously reported.<sup>30</sup> In the CD11c-DT conditional depletion model, the removal of CD11c+ DC (reaching 80%) prior to Sgca-HY gene transfer reduced anti-transgene CD4<sup>+</sup> T-cell responses by 70% meaning that CD11c+ DC were essential to mount anti-transgene CD4-mediated immune responses (Figure 2a). Accordingly, CD11c+ DC efficiently presented transgenic epitopes to specific CD4<sup>+</sup> T cells following systemic administration of rAAV1-Sgca-HY (Figure 2b). In this model, CD11b+ cells were as efficient as CD11c+ cells to present transgenic CD4 T-cell epitopes, whereas CD19+ B cells were incapable of such activity (Figure 2b). Thus contrary to the capsid, both DC and macrophages can process and present the transgene product *in vivo*. Indeed, adoptive transfer of rAAV1-Sgca-HY-loaded CD11c+ or CD11b+ cells both successfully primed specific CD4<sup>+</sup> T cells (Figure 2c).

Sialic acids were involved in T-cell priming to the transgene since the injection of NA-treated and rAAV1-loaded CD11c+ or CD11b+ cells induced lower levels of anti-transgene CD4-mediated immune responses compared to non-NA-treated control cells (Figure 2c). The serotype specificity of the NA-digestion was confirmed with the use of rAAV8, a serotype which does not bind cells through sialic acid recognition. Contrary to rAAV1, rAAV8 was capable of inducing anti-transgene T-cell immune responses in our model regardless of NA digestion (Supplementary Figure S1c). Those data point out the central role played by sialic acids on CD11c+ DC and CD11b+ macrophages in the immunogenicity of the transgene when delivered by rAAV1.

### Sialic acid binding enables rAAV1 targeting of macrophages and CD11c+CD8 $\alpha$ + DC

Having established that sialic acids on CD11c+ DC and CD11b+ macrophages contribute to the overall immunogenicity of the vector, we investigated if sialic acids confer a specific pattern of interaction between rAAV1 and APCs *in vivo* as compared to inert particles. Twenty nanometers of carboxy-functionalized polystyrene fluorescent nanospheres were chosen for similar physical characteristics to rAAV in general and were therefore expected to indicate levels of serotype-non-specific interactions with APCs. To detect serotype-specific interactions, rAAV1 particles were marked with fluorochromes enabling the detection by flow cytometry (fluorescence activated cell sorting (FACS)) of cells interacting with the vector in the organs of mice with similar sensitivity as for inert particles. Following IV injection, both fluorescent rAAV1 and fluorescent nanospheres were found within all the splenic APC populations tested (including various subpopulations of CD11c+ DC, CD11b+ macrophages, and CD19+ B cells—Supplementary Figure S2a) but with obvious differences (Figure 3a–d). The injected viral or inert particles interacted with less than 8% of CD19+ B cells without selective preference between the viral or inert particle (Figure 3a). In contrast to B cells, both CD11c+ DC and CD11b+ macrophages interacted more with rAAV1 than with nanospheres (Figure 3a) suggesting that specific interactions

occur between the vector and these cells. Within the CD11c+ DC population, the CD8 $\alpha$ + CD11c+ subpopulation was twice more targeted by rAAV1 than by nanospheres whereas CD11c+CD11b+ DC or CD11c+pDca+ pDC subpopulations did not exhibit this preference (Figure 3b). Strikingly, CD11b+F4/80+ macrophages interacted far more efficiently with rAAV1 than with nanospheres

(five to six times more) and with high efficiency since more than 70% of the cells were targeted (Figure 3c). Using another fluorescent marker, we confirmed that the monocytic/macrophagic population, stained as Gr1<sup>int</sup> cells, was preferentially targeted by rAAV1 as compared to nanospheres (Figure 3c). These interactions were not only observed in the spleen but also in the liver

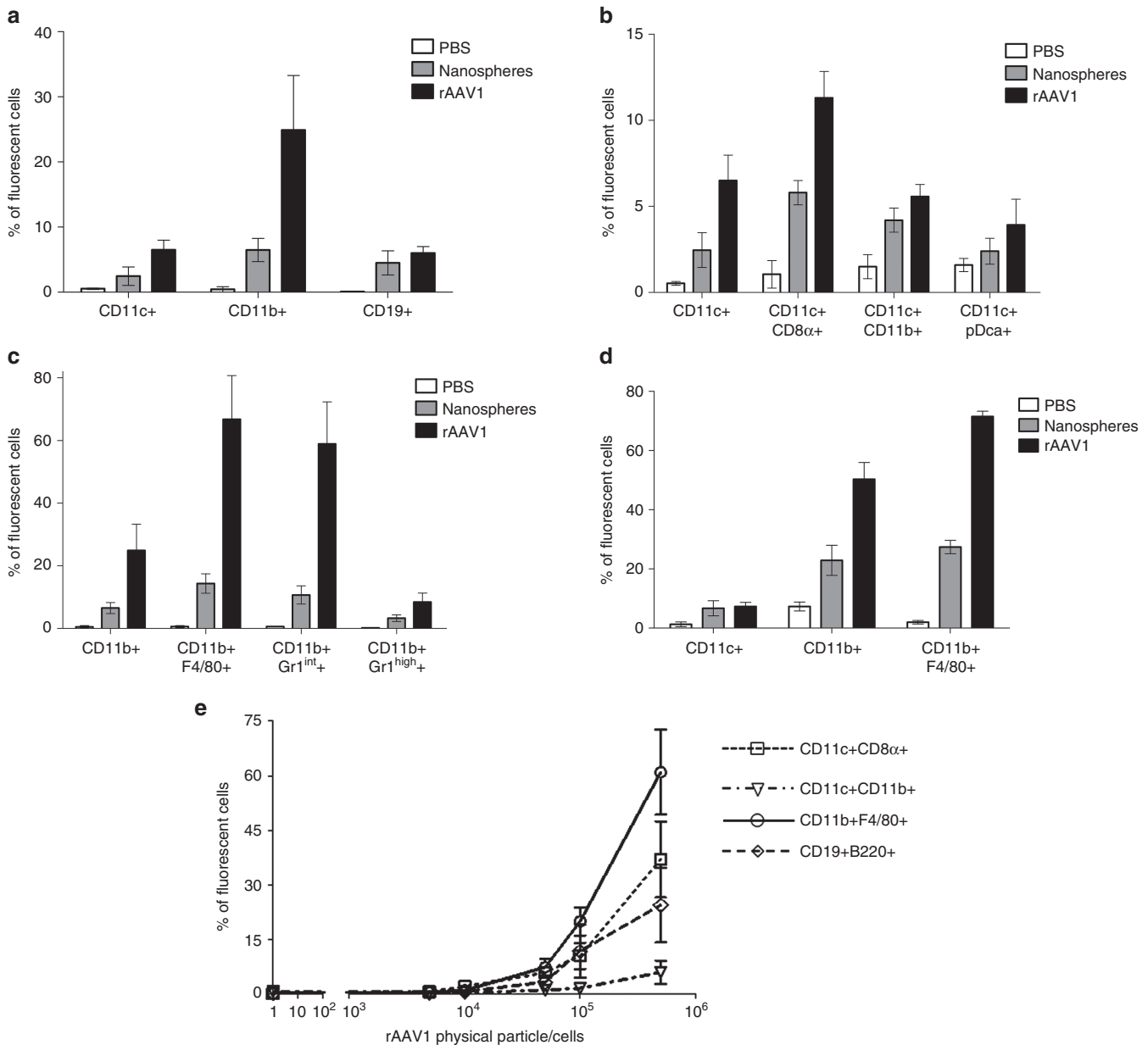


**Figure 3** Antigen-presenting cells (APCs) targeting by rAAV1. (a–d) C57BL/6 mice were injected IV in the retro-orbital sinus with  $10^{13}$  pp of nanospheres (gray bars) or same amount of Alexa Fluor-labeled rAAV1 (black bars) or with equivalent volume (100  $\mu$ l) of phosphate-buffered saline (PBS) (open bars). Two hours later, various populations of cells were sorted with magnetic beads from the spleen (CD11c+, CD11b+, CD19+ cells) (as indicated in **Supplementary Figure S2a**) or from the liver (CD45+ cells) of mice to measure the presence of fluorescent particles by FACS. Prior to FACS analysis, sorted cells were stained with noninterfering fluorescence to recognize the CD8 $\alpha$ , CD11b, pDC, F4/80, and Gr1 subsets. Data are expressed as the mean percentage of fluorescent cells  $\pm$  SD obtained in three independent experiments, each including two or three mice per group, testing two different batches of rAAV1. Measures of particle targeting were made: (a) in total spleen CD11c+ CD11b+ and CD19+ cells (b) in subsets of the sorted CD11c+ spleen cells as identified by multi-color staining as indicated (c) in subsets of the sorted CD11b+ spleen cells as identified by multi-color staining (d) in subsets of the sorted liver CD45+ cells identified by multi-color staining. (e) *In vitro* rAAV1 binding assay. Splenic CD11c+, CD11b+, and CD19+ cells were obtained from untreated C57BL/6 mice using the same purification technique as above and cells were incubated 1 hour at 4  $^{\circ}$ C with different amounts of Alexa-fluor 488-stained rAAV1 vector and the percentage of fluorescent cells was measured by FACS. Data are representative of one experiment out of five. FACS, fluorescence activated cell sorting.

(Figure 3d). *In vitro*, rAAV1 also preferentially interacted with F4/80+ macrophages at any of the concentration tested (Figure 3e), and to a lower extent with CD8 $\alpha$ + CD11c+ DC and B cells. CD11c+ CD11b+ cells were poorly targeted.

To determine if sialic acids might account for the differential interactions between rAAV1 and APCs, cells were treated with NA and tested for binding to fluorescent rAAV1. Efficient enzymatic digestion by NA was confirmed using a fluorescent Wheat germ agglutinin (WGA) lectin which binds  $\alpha$ 2,3  $\alpha$ 2,6  $\alpha$ 2,8  $\alpha$ 2,9 N-acetylglucosamine linkage (Supplementary Figure S2b). The NA treatment significantly reduced the number of rAAV1-positive F4/80+ macrophages compared to nontreated cells (by about 30%) and CD8 $\alpha$ + CD11c+ DC (by about 40%) (Figure 4a), confirming the involvement of sialic acids in the binding of rAAV1 by those cells. In contrast, the overall binding of rAAV1 to B cells was not affected by removing sialic acids (Figure 4a).

Competition experiments were performed to better characterize the importance of different sialic acid linkages in

the interactions between rAAV1 and the different cell types. Competition between labeled rAAV1 and increasing doses of fluorescent lectins: Maackia Amurensis agglutinin (MAA), Sambucus Nigra agglutinin (SNA), and WGA detect respectively  $\alpha$ 2,3-linked sialic acids,  $\alpha$ 2,6-linked sialic acids or all linkages. At low doses of WGA, rAAV1 competes better for binding on CD8 $\alpha$ + CD11c+DC as compared to F4/80+ macrophages. With increasing doses of WGA, a dose-effect was clearly seen for F4/80+ macrophages (Figure 4b). Both MAA and SNA competed for the binding of rAAV1 to CD8 $\alpha$ + CD11c+DC, while the competition with SNA on F4/80+ macrophages was marginal as compared to MAA. The results argue that  $\alpha$ -2,3-N-sialic acids on macrophages predominantly contribute to the interactions with rAAV1 whereas both  $\alpha$ -2,3- and  $\alpha$ -2,6-N-sialic acids contribute to a similar extent on CD8 $\alpha$ +CD11c+DC. Regarding B cells, both WGA and SNA but not MAA significantly competed for rAAV1 binding, suggesting that  $\alpha$ -2,6-N-sialic acids on B cells have the ability to interact with

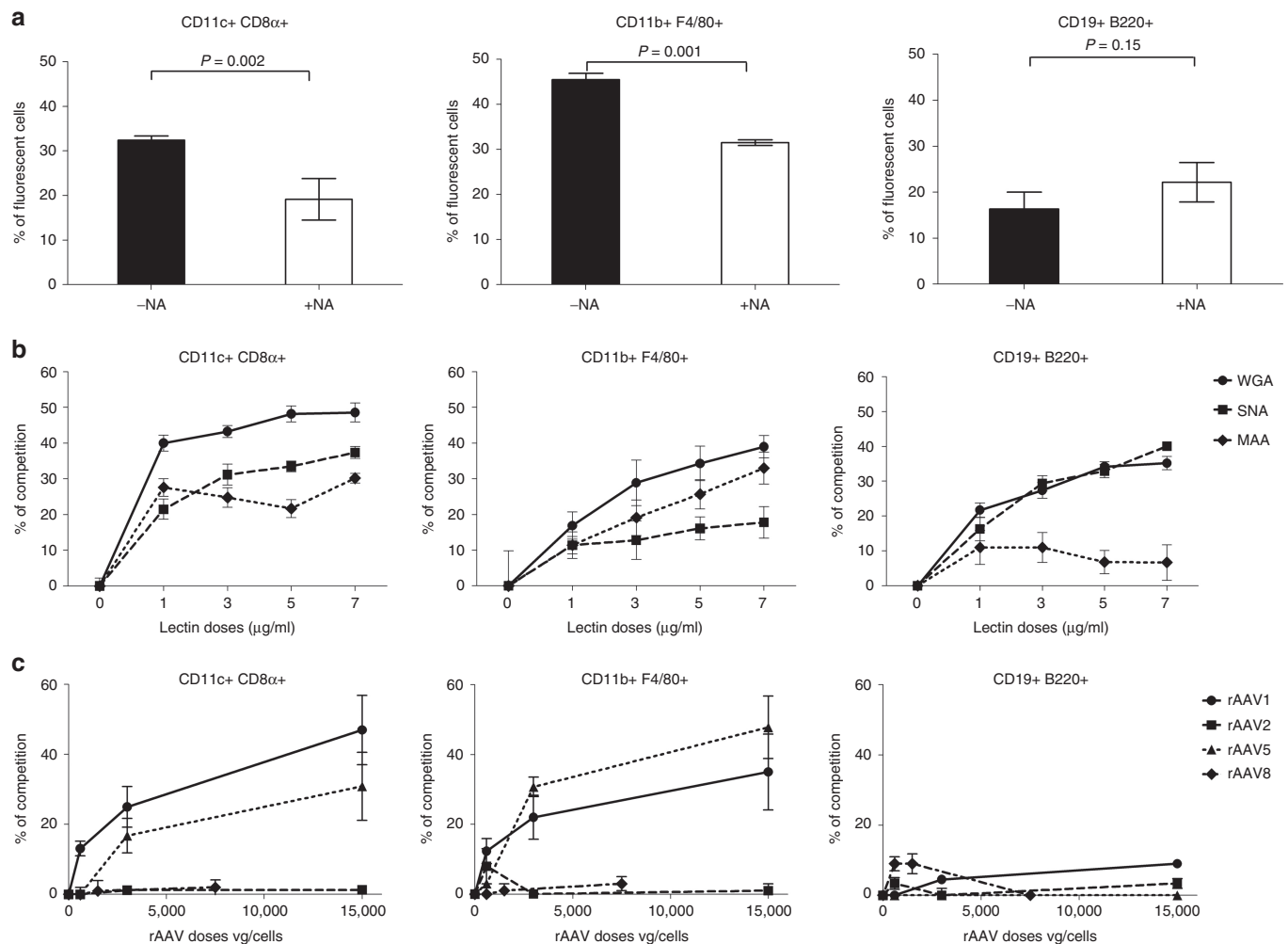


**Figure 4** Involvement of sialic acids in rAAV1 binding to macrophages and DC. Antigen-presenting cells (APCs) obtained as indicated in Figure 3e underwent various treatments before measuring *in vitro* the binding of fluorescent rAAV1 using multi-color FACS. *In vitro* binding with fluorescent rAAV1 was measured: (a) after treatment of the cells with NA, (b) after competition with increasing doses of fluorescent lectins: Wheat germ agglutinin (circle), Sambucus Nigra agglutinin (square) or Maackia Amurensis agglutinin (diamond-shaped), (c) after competition with various capsid serotypes. Results on CD11c+ CD8 $\alpha$ + DC, CD11b+ F4/80+ macrophages, and CD19+ B220+ B cells are represented respectively in the left, middle and right panels. Results represent the average percentage values  $\pm$  SD in three to four independent experiments. FACS, fluorescence activated cell sorting.

rAAV1 even though sialic acid-independent mechanisms seemed to play a major contribution in these cells.

Then, to assess if other properties shared by rAAV vectors could explain part of the binding specificity of rAAV1 on these cells, we performed competition assays between labeled rAAV1 and nonlabeled vectors using different capsid serotypes (1, 2, 5, and 8) known to utilize different cell entry receptors.<sup>25,31,32</sup> As shown in **Figure 4c**, binding of rAAV1 to F4/80+ macrophages and CD8 $\alpha$ + CD11c+DC competed in a dose-dependent manner with itself and with rAAV5 but neither with rAAV2 nor rAAV8. Therefore, these data confirmed that binding of rAAV1 to APC is sialic acid dependent since rAAV1 shares with rAAV5 the ability to bind  $\alpha$ -2,3-N-sialic acids, but no other shared binding specificity emerged.

Thus, primary receptors described for the rAAV1 vector mediate its binding to CD8 $\alpha$ + CD11c+DC and to F4/80+ macrophages and explain the greater tropism of rAAV1 for those cells *in vivo* as compared to nanospheres.

### Sialic acid-independent signals provided by the structure of rAAV1 are sufficient to recruit and to activate APC

AAV1 may not only provide antigens by targeting APC in a sialic acid-dependent manner, but could also deliver signals to recruit and activate those cells. As shown in **Figure 5a–c**, the systemic administration of rAAV1 caused selective changes in cell populations of the spleen at early time points (2 hours). Injections of rAAV1 did not modify splenic CD11c+ DC subpopulations (**Figure 5a**), but increased by three-fold the relative number of CD11b+F4/80+SSC<sup>low</sup> and the CD11b+Gr1<sup>int</sup>SSC<sup>low</sup> cells among the CD11b+CD11c- population with no change in the CD11b+Gr1<sup>high</sup> cells (**Figure 5b,c**). Injection of the same amount of nanospheres provided the same results, meaning that changes observed in monocytes/macrophages proportions in the spleen are not due to signals triggered upon sialic acids recognition, but presumably by the nanoparticulate nature of rAAV1. The same was observed in liver (data not shown).

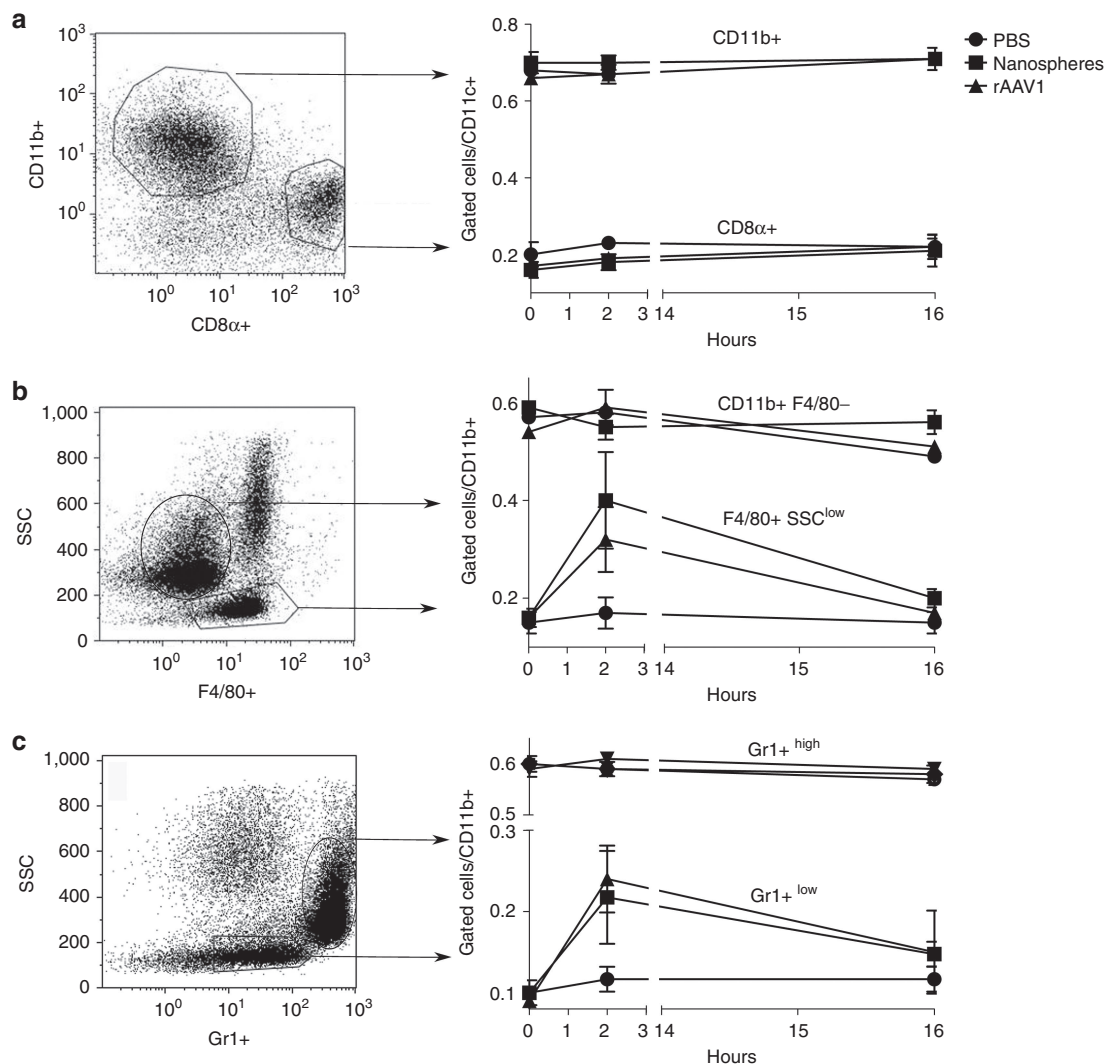


**Figure 5** Antigen-presenting cell (APC) mobilization by rAAV1 vector and nanospheres. C57BL/6 mice were injected as in Figure 3a and spleens were harvested 2 or 16 hours later to select CD11c+ (**a**) and CD11b+ (**b** and **c**) cells by magnetic cell sorting followed by multi-color stain and FACS analysis. The percentage of cell subsets in the represented gates in response to rAAV1 or nanospheres injection (left scatter plots) are averaged  $\pm$  SD in three independent experiments, each including three mice per group, testing two different batches of rAAV1 and are represented in the right line graphs. FACS, fluorescence activated cell sorting.

To analyze if interactions with particles activate APC, we compared the cellular expression of MHC II, costimulatory molecules (CD80, CD86), CD206 and CD301 markers following administration of fluorescent nanospheres or of fluorescent rAAV1. **Supplementary Figure S3** shows the level of expression of each individual cellular marker in populations of cells positive or negative for beads or for rAAV1. In parallel to serve as controls, mice were injected with phosphate-buffered saline (PBS) or with agonists for TLR4 and TLR9, *i.e.*, LPS and CpG A, CpG B which are known to activate APC *in vivo* but with different efficacy. Results on the percentage and the level of expression for each of these parameters were integrated in a multiparametric analysis using principal component analysis (PCA) followed by hierarchical clustering. This analysis clearly distinguished DC or macrophages harvested from PBS-injected mice from those obtained from CpG- or LPS-injected mice (**Figure 6**; **Supplementary Figure S4**). Interestingly, PCA distinguished the effects of beads and of rAAV1 from the effects of PBS both in DC and macrophages (**Figure 6**). This observation was confirmed by hierarchical clustering (**Supplementary Figure S4**) and by statistical analysis on PC1 which captures approximately 70% of data (**Table 3**). Indeed, statistical significance is found between DC from PBS- and rAAV1-injected mice ( $P = 0.001$ ), but not between DC from nanosphere- and rAAV1-treated mice ( $P = 0.087$ ). Similar clear cut observations were made for the CD11b+ macrophagic population ( $P = 0.0002$  for *t*-test (PBS, rAAV1), and  $P = 0.4$  for *t*-test (nanosphere, rAAV1)).

Such data showed that the recruitment of macrophages and the activation pattern of DC and macrophages are similarly induced by inert and by viral particles. The sheer nano-particulate structure of rAAV can therefore contribute to immunize in addition to specific interactions that will occur with APCs. The

immunogenicity induced by the administration of rAAV1 gene transfer vectors is therefore complex and involves various properties of the vector itself, associated with the existence of diverse APCs with differential ability to interact with vectors as summarized in **Table 4**, contributing to explain the differential T-cell immunization against capsid and transgene.

## DISCUSSION

In this study, we provide evidence for the first time that the rAAV1 serotype-specific sialic acid receptors on APCs and nonspecific properties inherent to the vector as a nanoparticle, can both contribute to immune responses induced by gene transfer *in vivo*. While several prior studies have shown that rAAV can transduce human or murine DCs *in vitro* or *in vivo*, triggering CD8<sup>+</sup> T cells or the production of inflammatory cytokines,<sup>19–21,33–37</sup> our study is the first to explore in detail the complex *in vivo* interactions between rAAV1 and diverse populations of APCs to understand the basis of anti-transgene and anti-capsid T-cell immunity particularly in the case of CD4<sup>+</sup> T-cell responses.

Viral vectors like rAAV are nanoparticles and physicochemical properties of nanoparticles like size, surface chemistry, charge, are known to play a crucial role in their interactions with cells and with the immune system *in vivo*.<sup>38</sup> The size of the particles is known to directly modulate APC function and activation thresholds.<sup>39,40</sup> Strong signals are provided by positively charged nanoparticles induce systemic toxicity and Th1 immune activation through TLR4.<sup>41</sup> While cationic polystyrene nanoparticles induce toxic oxidative stress, to activate the NLRP3 inflammasome and the subsequent release of proinflammatory cytokines in macrophages, anionic and neutral nanoparticles do not have such effects.<sup>42</sup> While the exact physicochemical characteristics of rAAV

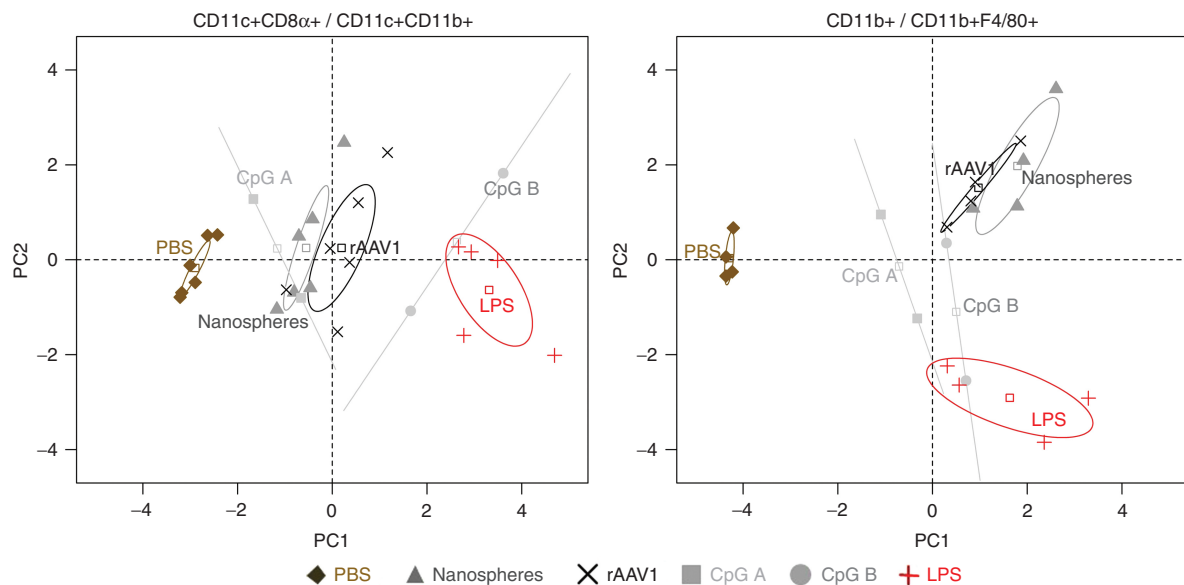


**Figure 6** Analysis of antigen-presenting cell (APC) activation by rAAV1 using principal component analysis (PCA). Mice were injected IV with phosphate-buffered saline (PBS) (diamond), rAAV1 (X), nanospheres (triangle), CpG A (75 µg/mice) (gray square), CpG B (75 µg/mice) (gray circle), and LPS (5 µg/mice) (plus sign). Spleens were harvested 16 hours later and CD11c+ and CD11b+ cell subsets were magnetically-sorted, stained with antibodies to CD8α, CD11b, F4/80, CD86, CD80, MHCII, CD301, and CD206 and analyzed by multi-color FACS. Data were submitted to PCA separating results for CD11c+ CD8α+ cells and CD11c+ CD11b+ cells (left plot) from results on CD11b+ cells and CD11b+ F4/80+ cells (right plot). For each treatment, each dot represents the integrated value calculated by PCA and the 95% confidence interval is represented by an ellipse. Data include three experiments, each including three mice per group. FACS, fluorescence activated cell sorting; LPS, lipopolysaccharide.

preparations are not defined and not inferred from the present study, we observe that the level of immune cell activation produced by rAAV1 is similar to that of anionic nanoparticles comparable in size, in terms of inducing MHC II and costimulatory molecules (CD80, CD86) on conventional DC, or macrophages and clearly inferior to what could be provided by microbial signals such as TLR agonists. In addition, rAAV1 and nanoparticles, both induced the rapid mobilization of some CD11b+ cell subsets in the spleen (CD11b+F4/80+SSC<sup>low</sup> and CD11b+Gr1<sup>int</sup>SSC<sup>low</sup> cells). Taken together, this suggests that the nanoparticulate nature of AAV more than its serotype-dependent binding properties provides initial activation signals to APCs upon delivery. This serotype-non-specific effect may therefore not only diversify the populations of APCs recruited to the immune response following gene transfer but may also contribute to cellular activation signals received by APCs in addition to those transmitted by serotype-specific interactions or by TLR, C-type lectin receptors, or damage-associated molecular patterns. Additional signals provided by DNA or RNA are known to augment stimulation by virus-like particles.<sup>43</sup> In the case of rAAV, prior studies have implicated

TLR9 and CpG DNA in the immunogenicity of rAAV1, rAAV2, rAAV9 vectors and the transgene.<sup>44,45</sup> Our observations complete the understanding of innate immune system activation by rAAV administration and provide functional bases for further structure/function studies of rAAV.

Besides interactions determined by physicochemical properties of rAAV, specific molecular interactions also take place. Sialic acids play a clear role in targeting and delivering the rAAV1 vector to APCs. While this is not entirely unexpected considering the known tropism of the vector,<sup>25</sup> our study provides the first description of functional sialic acid-mediated interactions with CD11b+F4/80 macrophages and CD8 $\alpha$ + CD11c+ DC and shows the importance of this mechanism for anti-capsid and anti-transgene immune responses. Sialic acids not only play an important role in determining interactions of rAAV1 with conventional DC but also seem to favor the capacity to endocytose the vector which is coherent with prior studies with human immature DC.<sup>26</sup> However, contrary to DC, macrophages were really inefficient in presenting the vector capsid to CD4<sup>+</sup> T cells in spite of entry of rAAV1 in the cells as seen by confocal microscopy (**Supplementary Figure S5**). It is known that the phospholipase A2 activity of the capsid VP1 protein results in the partial escape of the particle from the endosomal route to the nucleus via the cytosol.<sup>46</sup> As a result, infection of APCs with rAAV probably induces processing of capsid antigens for presentation on MHC class II molecules not through the classical exogenous pathway but mainly through the endogenous route which is not efficient in macrophages.<sup>47</sup> However, since macrophages are highly targeted by rAAV1, these cells may play a major indirect role in transferring capsid antigens to immunocompetent cells such as DC. Indeed, we have shown that adoptive transfer of rAAV1-loaded CD11b+ cells in an immunocompetent host can trigger a CD4<sup>+</sup> T-cell-mediated anti-capsid immune response, suggesting that direct targeting of CD11c+ DC by the vector is not fully required. However, we can speculate that direct targeting of CD8 $\alpha$ + CD11c+ DC is important for cross-presentation of capsid determinants to CD8<sup>+</sup> T cells, since as opposed to CD8 $\alpha$ - CD11c+ DC, this population has the intrinsic ability to cross-present antigens.<sup>13</sup>

Conversely, both DC and macrophages were capable of presenting transgene determinants onto MHC II molecules, suggesting that they were efficiently transduced by the vector *in vivo*. Given the potent response against immunogenic transgene-encoded products, rAAV1 could be used as a direct source of

**Table 3** Statistical analysis of the principal component analysis results on two different types of APC

<b>a) CD11c+ and CD11c+CD8<math>\alpha</math>+ cells</b>					
	CpG B	CpG A	LPS	rAAV1	Beads
PBS	0.016	0.112	0.001	0.001	0.007
Beads	0.270	0.405	0.013	0.087	
rAAV1	0.435	0.050	0.157		
LPS	0.990	0.009			
CpG A	0.219				
<b>b) CD11b+ and CD11b+F4/80+ cells</b>					
	CpG B	CpG A	LPS	rAAV1	Beads
PBS	0.03	0.01	0.0004	0.0002	0.0002
Beads	0.16	0.21	0.006	0.37	
rAAV1	0.70	0.23	0.003		
LPS	0.86	0.05			
CpG A	0.18				

P values obtained from two-tailed Student's test analysis comparing two experimental groups (PBS, nanosphere, rAAV1, LPS, CpGA and CpGB) on PC1 for 2 different cell types: **a)** CD11c+ and CD11c+CD8 $\alpha$ + cells and **b)** CD11b+ and CD11b+F4/80+ cells.  
LPS, lipopolysaccharide; PBS, phosphate-buffered saline.

**Table 4** Diverse populations of antigen-presenting cells differentially interact with rAAV1 and differentially present transgene and capsid to induce T-cell responses

	Sialic acid involvement		Nanoparticulate structure contribution		Capsid		Transgene		
	Linkage	Binding of rAAV1	Antigenic presentation	Activation	Recruitment	Antigenic presentation of,	T-cell response to,	Antigenic presentation of,	T-cell response to,
Dendritic cells; CD11c+	$\alpha$ 2.3 and $\alpha$ 2.6	Yes, mainly on CD8 $\alpha$ +	Yes	Yes	No	Yes	Yes	Yes	Yes
Monocytes/macrophages; CD11b+	$\alpha$ 2.3	Yes, mainly on F4/80+	Yes	Yes	Yes	No	Yes	Yes	Yes
B lymphocytes; CD19+	$\alpha$ 2.6	No	No	Not tested	Not tested	No	Not tested	No	Not tested

DNA vaccine, or to transfer antigens to DC *ex vivo* for vaccination as it has been reported in cancer trials.<sup>3</sup> Interestingly, rAAV5 which shares with rAAV1 a receptor for  $\alpha 2-3$ , but not for  $\alpha 2-6$  N-linkages, has been described as the most potent serotype to transduce murine as well as human DC and induce maturation.<sup>21</sup> Because transgene products can be presented by macrophages following rAAV1 gene transfer suggests that sufficient amounts of encoded transgene product is generated in these cells in spite of the excessive degradation of endogenously produced proteins described in these cells,<sup>47</sup> and/or that other pathways favoring endogenous antigen presentation such as autophagy, were stimulated following rAAV1 transduction. The respective contribution of those pathways would be important to evaluate with specific rAAV serotypes since they depend upon the nature of the pathogen/stimuli involved. Our data support at least the first hypothesis since removal of sialic acids on CD11b+ cells by decreasing the entry of the particles dramatically reduced the immune response to the transgene upon adoptive transfer of rAAV1-loaded CD11b+. Sialic acids on DC were also essential to deliver sufficient amount of antigen to trigger potent anti-transgene and anti-capsid immune responses. However, the anti-capsid immune response seemed to be less dependent upon sialic acids than the anti-transgene immune response indicating a possible contribution of structural stimulating signals in the response of these cells. The partial depletion of DC reduced more significantly the anti-transgene than the anti-capsid immune response, highlighting the importance of this population of APCs in response to gene delivery by rAAV1.

Many viruses attach to cells via sialylated glycans and interactions with linked carbohydrates typically define the specificity, tropism, and affinity of viruses as shown in particular with Influenza.<sup>27</sup> Here, we focused on  $\alpha 2-3$  and  $\alpha 2-6$ -linked sialic acids since they are receptors for AAV1 and found different contributions on murine DC and macrophages which may impact immune responses against the capsid or transgene. Sialic acids can be differentially expressed in mice and human, and even human and closest evolutionary relatives display differences in the sialic acids biology.<sup>48</sup> Therefore, differences may exist between murine and human APCs in their interactions with rAAV1 and subsequent immune responses. It is known that the surface sialylation of DC is modulated according the cell differentiation and maturation.<sup>26</sup> In steady state, the pattern appears to be similar in mice and humans since in both species immature DC are highly sialylated and express  $\alpha 2-3$ - and  $\alpha 2-6$ -linked sialic acids. An accurate comparison of the sialic acid content and distribution on the same cells in mice and human is not available to our knowledge.

Thus, immunogenicity of rAAV is complex. In the context of gene therapy, preventing a direct access of the vector to APC would be recommended to limit the immunogenicity to the different components provided or encoded by the vector. Therefore, criteria for the selection of rAAV for gene transfer should consider the interaction between rAAV and APC particularly selecting new variants based on their tropism.

## MATERIALS AND METHODS

**Animals.** Mice were housed and bred in our accredited facility (French national agreement number C91.228.101). All animal experiments were

performed according to the institutional and international guidelines for animal care and use. Experimental procedures were performed in accordance with French and European directives, approved by the local ethical committee (C2EA-64) and Ministry of Research for gene-modified organism studies (agreement 5244-CAI). Six- to 8-week-old CD45.2+ C57BL/6 and congenic CD45.1+ C57BL/6 female mice were purchased from Charles River (Labresle, France and Calco Como, Italia respectively). Marilyn (CD45.1 Rag2<sup>-/-</sup>) mice whose CD4<sup>+</sup> T cells are specific for Dby/I-Ab were kindly provided by O. Lantz and bred in our animal facility. Hemizygous CD11c-DTR mice were purchased from Jackson Laboratory (Bar-harbor, ME) and intercrossed to obtain homozygous CD11c-DTR which were then bred in our animal facility and used in the experiments. To obtain CD11c-DTR expression on hematopoietic cells only, chimeric CD11c-DTR female mice were created by transferring  $5 \times 10^6$  bone marrow cells harvested after flushing cells from tibia and femur of CD11c-DTR female mice into lethally irradiated (9,5 gray) congenic CD45.1+ C57BL/6 female mice. The reconstitution was attested by measuring blood cell counts using the MS9 counter (Melet Schloesing Laboratories, Osny, France) and the percentage of chimerism was evaluated by the CD45.1/CD45.2 ratio in the live cell gate using flow cytometry.

**Peptides, rAAV vectors, and nanospheres.** The Dby peptide was synthesized by Genepep (Montpellier, France). All rAAV used in the study were nonreplicative adenovirus-free viral preparations prepared by transient tri-transfection of HEK293T cells using endotoxin-free plasmids (Macherey-Nagel, Hoerd, France). All vectors were purified by centrifugation over a CsCl gradient and titered in viral genome (vg) by real-time PCR. Vector final suspensions were tested for endotoxin level and found to be < 10 EU/ml. The rAAV1-DBY vector was described previously.<sup>24</sup> Various serotypes of rAAV (rAAV1, rAAV2, rAAV5, and rAAV8) were produced as described<sup>49</sup> using various transgene constructs described elsewhere<sup>24,50</sup>: pGG1 SGCA\_HY for rAAV1; pGG2-CMV-muSEAP for rAAV2 and rAAV5; pU7\_DTex23 for rAAV8. For fluorescent labeling of rAAV1, covalent staining with Alexa-fluor 488 or Alexa-fluor 633 was performed using a labeling kit according to the manufacturer's instructions (Invitrogen, Carlsbad, CA). The concentration of rAAV1 particles (pp/ml) was evaluated by ELISA (Progen, Heidelberg, Germany).

Nanospheres consisted of yellow-green 20 nm carboxylate-modified ultraclean polystyrene fluospheres and the stock particle concentration was indicated by the manufacturer (Invitrogen).

**Lectins, neuraminidase, and diphtheria toxin.** WGA, SNA, and MAA (Biovalley SA, Marne La Vallée, France) bind to sialic acid recognizing either all linkages (WGA), Neu5Ac $\alpha 2-6$ Gal(NAc)-R (SNA) or Neu5Ac/Gc $\alpha 2,3$ Gal $\beta 1,4$ GlcNAc/Glc (MAA) motifs. The lectins were conjugated to fluorescein isothiocyanate by the manufacturer and the stock solution (5 mg/ml) was reconstituted according to the instructions and stored at  $-20^{\circ}\text{C}$ .

Neuraminidase (NA) from *Vibrio cholerae* (Sigma-Aldrich, St. Louis, MO) was used to hydrolyze Neu5A  $\alpha 2,3$ ,  $\alpha 2,6$ , and  $\alpha 2,8$  linkages. For the treatment, CD11c+, CD11b+, and CD19+ cells were incubated 2 hours at  $37^{\circ}\text{C}$  with 50 mU/mg of NA in PBS 1 $\times$ , Ca<sup>2+</sup>, Mg<sup>2+</sup>.

Corynebacterium diphtheriae diphtheria toxin unnicked (DT) (Calbiochem-Millipore, Billerica, MA) was used to deplete CD11c+ cells in chimeric CD11c-DTR mice. Mice were injected intraperitoneally (IP) three times every 2 days with 1  $\mu\text{g}/\text{ml}$  of DT diluted in PBS.

**Purification of APC by magnetic cell sorting.** Spleens were harvested from naive mice for *in vitro* experiments or from IV-injected mice for *ex vivo* experiments. CD11c+, CD11b+, and CD19+ cells were obtained as previously described.<sup>51</sup> CD11c+ cells were collected from these spleen digested first with collagenase IV (Invitrogen), DNase I (Roche Diagnostics, Meylan, France), incubated with anti-CD11c-magnetic beads (Miltenyi Biotec, Paris, France) and purified by automatic magnetic cell sorting (AutoMACS, Miltenyi Biotec). Cell purity ranged from 93 to 97%. The residual unselected cells were labeled with anti-CD11b-magnetic beads

(Miltenyi Biotec) to purify CD11b+ cells reaching a purity ranging from 85 to 90%. B lymphocytes were obtained from residual unselected cells from these two prior processes (*i.e.*, CD11c- CD11b- cells) using anti-CD19-magnetic beads positive selection. The purity was 98%. AutoMACS programs POSSELD(S) or POSSELD were used for CD11c+ cells positive selection, POSSELD for CD11b+ cells positive selection, and POSSEL for CD19+ cells positive selection. For *ex vivo* cell binding experiments, preparations of CD45+ cells were obtained from liver following digestion of the organ with collagenase IV (Invitrogen), DNase I (Roche Diagnostics). Cells were obtained by positive selection using anti-CD45-magnetic beads (Miltenyi Biotec) and automatic magnetic cell sorting (POSSEL program, AutoMACS, Miltenyi Biotec). The purity was 97%.

**Competition assays with rAAV serotypes and lectins.** To performed competitions assays,  $10^6$  CD11c+, CD11b+, and CD19+ cells were incubated at 4 °C with fluorescein isothiocyanate-conjugated lectins (1, 3, 5, 7 µg/ml) or with rAAV with capsid serotypes 1, 2, 5, and 8. Batches of vector used for the study had the following titers: rAAV5 CMV-mseap:  $7.7 \times 10^{11}$  vg/ml; rAAV1 SGCA-HY:  $6 \times 10^{11}$  vg/ml; rAAV2 CMV mseap:  $5.3 \times 10^{11}$  vg/ml; rAAV8 pU7\_DTex23:  $2.3 \times 10^{12}$  vg/ml. After 10 minutes,  $10^3$  vg/cells of Alexa fluor-stained rAAV1, corresponding to the EC50 dose, were added. One hour later, cells were extensively washed, resuspended in PBS, and stained. The competition assay was assessed by FACS by estimating the percentage of Alexa-fluor stained cells. And the percentage of competition was calculated as follows ((positive cells w/o competitor – positive cells w/o competitor)/positive cells w/o competitor). Analyses were performed on a LSRII using Diva software (BD-Biosciences, Le Pont de Claix, France).

**Ex vivo antigenic presentation to specific CD4+ T cells.** For *ex vivo* antigenic presentation, at least three mice per group were injected IV with the different rAAV1 vectors tested or with PBS as control and after 3–5 days (to examine capsid or transgene presentation, respectively), spleen cells were collected and CD11c+, CD11b+, and CD19+ cells were purified by automatic magnetic cell sorting (AutoMACS, Miltenyi Biotec). To analyze the antigenic presentation of Dby-specific CD4+ T cells were purified from Marilyn mice with anti-CD90.2-magnetic beads (Miltenyi Biotec) and then stained with carboxyfluorescein succinimidyl ester (CFSE) (Molecular Probes, Cambridge, UK) (2 µmol/l) in RPMI-1640 (Life Technologies, Carlsbad, CA) ( $10^7$  cells/ml) at RT for 8 and 2 minutes at 37 °C. The reaction was stopped by adding an equal volume of RPMI 1640 10% fetal calf serum (FCS) followed by 5 minutes incubation at 4 °C. Cells were extensively washed, resuspended in PBS, and put together with the CD11c+, CD11b+, and CD19+ cells at different APC:T cell ratio (1:25,000; 1:50,000; 1:75,000; 1:100,000) in a 96-well flat-bottom plate-Nunc (Dutcher, Brumath, France). Three days later, the CD4+ T-cell proliferation was assessed by FACS by estimating the CFSE dilution in CD4+ stained cells, and we calculated the % of dividing cells as follows: ((number of total cells – number of nondividing cells) × 100)/number of total cells). Analyses were performed on LSRII using Diva software (BD-Biosciences). Negative (CD11c+ + PBS) and positive (CD11c+ + Dby) controls were always included to assess the proliferation level.

**Immunostaining and flow cytometry.** All reagents used for flow cytometry were purchased from BD-Biosciences (Le Pont de Claix, France) and from e-biosciences (San Diego, CA) unless otherwise indicated. Cell suspensions were first incubated with anti-Fc $\alpha$ R1III/II (2.4G2) monoclonal antibodies (mAb) for 15 minutes at 4 °C and then stained for 30 minutes at 4 °C in PBS with 0.1% bovine serum albumin (BSA) using saturating amounts of the following mAbs: pacific blue-conjugated anti-CD4; biotinylated-anti-CD11c, anti-CD11b, anti-F4/80 and PE-Cy7-conjugated streptavidin; PE-conjugated anti-pDca, anti-CD8 $\alpha$ , anti-CD11b; V450-conjugated anti-CD86; Alexa 647-conjugated anti-CD301; alexa 700-conjugated anti-MHCII; APC-conjugated anti-CD80; biotinylated-anti-CD206 (Abd Serotec, Kidlington, UK); and APC-Cy7-conjugated streptavidin. Dead cells were excluded using 7-amino-actinomycin D (0.3 mg/ml)

(Sigma-Aldrich) staining. Acquisitions were performed on a LSRII using Diva software (BD Biosciences) and analyses were carried out with Kaluza software (Beckman-Coulter, Villepinte, France).

**Adoptive transfer.** For adoptive transfer experiments, C57BL/6 mice were injected with  $10^6$  CD11c+ or CD11b+ cells digested or not with NA and pulsed *in vitro* with  $5.10^3$  vg/cell of rAAV1 vectors or PBS as control. Each mouse was injected IV in retro-orbital sinus with 100 µl of cells preparation.

**Vector intramuscular injections.** For IM injection of vector, animals were anesthetized by intraperitoneal injection of xylazine (10 mg/kg) and ketamine (100 mg/kg) and 25 µl of the viral preparation adjusted at the specified concentration was injected in the left tibialis anterior (TA). Mice were sacrificed at day 8 for the anti-capsid immune responses and at day 14 for the anti-transgene immune responses.

**Determination of the immune response by enzyme-linked immunospot assays.** IFN- $\gamma$  enzyme-linked immunospot assays were performed as previously described,<sup>30</sup> by culturing  $10^6$  spleen cells per well with or without 1 µmol/l of Dby peptide. As a positive control, cells were stimulated with Concanavalin A (Sigma-Aldrich) (5µg/ml). After 24 hours, spots were revealed and counted using an AID reader (Cepheid Benelux, Louven, Belgium). Spot forming units (SFU) per million cells are represented after subtraction of background values obtained with nonpulsed splenocytes.

**PCA and hierarchical clustering.** Cell surface expression of CD86, CD80, MHCII, CD301, and CD206 was measured by FACS on different populations of APC that were extracted from the spleen following administration of rAAV1, nanosphere, CpGA (ODN 2336, TLR-4 ligand), CpGB (ODN 10103, TLR-9 ligand) (Cayla Invivogen, Toulouse, France), or lipopolysaccharide (LPS) (Invitrogen). Marking was described by the percentage of positive cells, by the median and geometric mean of fluorescence in the positive cell population. Multiparametric database included the treatment condition, the replicate, and variables measured for each marker of interest. PCA was performed using the free R software (Vers.2.15.2)<sup>52</sup> and the FactoMineR package (Vers.1.26)<sup>53</sup> to visualize patterns in the data. The method consists in a dimension reduction that produces new uncorrelated variables from the linear association of original ones. First and second new computed dimensions catch most of the inertia contained in the data and are used in each PCA plot. Ellipses in PCA plots show the 95% confidence interval of the center of gravity of each treatment obtained in three independent experiments. Hierarchical clustering was performed on the principle components using the default parameters of the R package FactoMineR. The distances are computed using an Euclidean metrics and the tree aggregated using a complete linkage method. CD11c+ cells and CD11b+ cell subsets were analyzed as two separated data sets. For each set of data, a plot representing each individual and the associated variables plot are shown.

**Statistical analysis.** For PCA analysis, comparisons between two experimental groups were performed using unpaired two-tailed Student's test analysis. Apart from PCA studies, data were formatted with GraphPad Prism software (GraphPad, La Jolla, CA). Comparisons between two experimental groups were performed using a Mann and Whitney two-tailed analysis. *P* value under 0.05 was considered statistically significant. In the graphs, \**P* value inferior to 0.05, \*\*inferior to 0.01, and \*\*\*inferior to 0.001.

## SUPPLEMENTARY MATERIAL

**Figure S1.** Antigenic presentation and T cell activation controls.

**Figure S2.** Gating strategies and control of acid sialic removal on CD11c+CD8 $\alpha$ + and CD11b+F4/80+.

**Figure S3.** Activation of APCs by rAAV1 and nanospheres.

**Figure S4.** Clustering representation of PCA.

**Figure S5.** Confocal microscopy analysis showing the presence of rAAV1 in macrophages.

## ACKNOWLEDGMENTS

The authors are grateful for the technical help from Cyril Wilmes and for support from the vector core, bioexperimentation group and animal facility at Genethon. We thank the vector core of the University Hospital of Nantes for the production of the AAV1-DBY. This work was supported by funds from AFM/Telethon.

## REFERENCES

- Okada, T, Nonaka-Sarukawa, M, Uchibori, R, Kinoshita, K, Hayashita-Kinoh, H, Naitahara-Kasahara, Y *et al.* (2009). Scalable purification of adeno-associated virus serotype 1 (AAV1) and AAV8 vectors, using dual ion-exchange adsorptive membranes. *Hum Gene Ther* **20**: 1013–1021.
- Venkatakrishnan, B, Yarbrough, J, Domsic, J, Bennett, A, Bothner, B, Kozyreva, OG *et al.* (2013). Structure and dynamics of adeno-associated virus serotype 1 VP1-unique N-terminal domain and its role in capsid trafficking. *J Virol* **87**: 4974–4984.
- Di, L, Zhu, Y, Jia, J, Yu, J, Song, G, Zhang, J *et al.* (2012). Clinical safety of induced CTL infusion through recombinant adeno-associated virus-transfected dendritic cell vaccination in Chinese cancer patients. *Clin Transl Oncol* **14**: 675–681.
- Trabelsi, K, Kamen, A and Kallel, H (2014). Development of a vectored vaccine against hepatitis E virus. *Vaccine* **32**: 2808–2811.
- Mingozzi, F and High, KA (2013). Immune responses to AAV vectors: overcoming barriers to successful gene therapy. *Blood* **122**: 23–36.
- Logan, GJ and Alexander, IE (2012). Adeno-associated virus vectors: immunobiology and potential use for immune modulation. *Curr Gene Ther* **12**: 333–343.
- Mueller, C, Chulay, JD, Trapnell, BC, Humphries, M, Carey, B, Sandhaus, RA *et al.* (2013). Human Treg responses allow sustained recombinant adeno-associated virus-mediated transgene expression. *J Clin Invest* **123**: 5310–5318.
- Ferreira, V, Twisk, J, Kwikkers, K, Aronica, E, Brisson, D, Methot, J *et al.* (2014). Immune responses to intramuscular administration of alipogene tiparovec (AAV1-LPL(S447X)) in a phase II clinical trial of lipoprotein lipase deficiency gene therapy. *Hum Gene Ther* **25**: 180–188.
- Haurigot, V, Mingozzi, F, Buchlis, G, Hui, DJ, Chen, Y, Basner-Tschakarjan, E *et al.* (2010). Safety of AAV factor IX peripheral transvenular gene delivery to muscle in hemophilia B dogs. *Mol Ther* **18**: 1318–1329.
- Gregory, AE, Titball, R and Williamson, D (2013). Vaccine delivery using nanoparticles. *Front Cell Infect Microbiol* **3**: 13.
- Cruz, LJ, Tacken, PJ, Rueda, F, Domingo, JC, Albericio, F and Figdor, CG (2012). Targeting nanoparticles to dendritic cells for immunotherapy. *Methods Enzymol* **509**: 143–163.
- Klippstein, R and Pozo, D (2010). Nanotechnology-based manipulation of dendritic cells for enhanced immunotherapy strategies. *Nanomedicine* **6**: 523–529.
- Mildner, A and Jung, S (2014). Development and function of dendritic cell subsets. *Immunity* **40**: 642–656.
- Pulendran, B (2015). The varieties of immunological experience: of pathogens, stress, and dendritic cells. *Annu Rev Immunol* **33**: 563–606.
- Bakdash, G, Sittig, SP, van Dijk, T, Figdor, CG and de Vries, IJ (2013). The nature of activatory and tolerogenic dendritic cell-derived signal II. *Front Immunol* **4**: 53.
- Archambault, AS, Carrero, JA, Barnett, LG, McGee, NG, Sim, J, Wright, JO *et al.* (2013). Cutting edge: Conditional MHC class II expression reveals a limited role for B cell antigen presentation in primary and secondary CD4 T cell responses. *J Immunol* **191**: 545–550.
- Martinez-Pomares, L and Gordon, S (2012). CD169+ macrophages at the crossroads of antigen presentation. *Trends Immunol* **33**: 66–70.
- Morva, A, Lemoine, S, Achour, A, Pers, JO, Youinou, P and Jamin, C (2012). Maturation and function of human dendritic cells are regulated by B lymphocytes. *Blood* **119**: 106–114.
- Gernoux, G, Guilbaud, M, Dubreil, L, Larcher, T, Babarit, C, Ledevin, M *et al.* (2015). Early interaction of adeno-associated virus serotype 8 vector with the host immune system following intramuscular delivery results in weak but detectable lymphocyte and dendritic cell transduction. *Hum Gene Ther* **26**: 1–13.
- Ferrand, M, Galy, A and Boisgerault, F (2014). A dystrophic muscle broadens the contribution and activation of immune cells reacting to rAAV gene transfer. *Gene Ther* **21**: 828–839.
- Xin, KQ, Mizukami, H, Urabe, M, Toda, Y, Shinoda, K, Yoshida, A *et al.* (2006). Induction of robust immune responses against human immunodeficiency virus is supported by the inherent tropism of adeno-associated virus type 5 for dendritic cells. *J Virol* **80**: 11899–11910.
- Martino, AT, Suzuki, M, Markusic, DM, Zolotukhin, I, Ryals, RC, Moghimi, B *et al.* (2011). The genome of self-complementary adeno-associated viral vectors increases Toll-like receptor 9-dependent innate immune responses in the liver. *Blood* **117**: 6459–6468.
- Fougerousse, F, Bartoli, M, Poupiot, J, Arandel, L, Durand, M, Guerchet, N *et al.* (2007). Phenotypic correction of alpha-sarcoglycan deficiency by intra-arterial injection of a muscle-specific serotype 1 rAAV vector. *Mol Ther* **15**: 53–61.
- Sudres, M, Ciré, S, Vasseur, V, Brault, L, Da Rocha, S, Boisgerault, F *et al.* (2012). MyD88 signaling in B cells regulates the production of Th1-dependent antibodies to AAV. *Mol Ther* **20**: 1571–1581.
- Wu, Z, Miller, E, Agbandje-McKenna, M and Samulski, RJ (2006). Alpha2,3 and alpha2,6 N-linked sialic acids facilitate efficient binding and transduction by adeno-associated virus types 1 and 6. *J Virol* **80**: 9093–9103.
- Crespo, HJ, Lau, JT and Videira, PA (2013). Dendritic cells: a spot on sialic Acid. *Front Immunol* **4**: 491.
- Stencel-Baerenwald, JE, Reiss, K, Reiter, DM, Stehle, T and Dermody, TS (2014). The sweet spot: defining virus-sialic acid interactions. *Nat Rev Microbiol* **12**: 739–749.
- Trottein, F, Schaffer, L, Ivanov, S, Paget, C, Vendeville, C, Cazet, A *et al.* (2009). Glycosyltransferase and sulfotransferase gene expression profiles in human monocytes, dendritic cells and macrophages. *Glycoconj J* **26**: 1259–1274.
- Jung, S, Unutmaz, D, Wong, P, Sano, G, De los Santos, K, Sparwasser, T *et al.* (2002). *In vivo* depletion of CD11c+ dendritic cells abrogates priming of CD8+ T cells by exogenous cell-associated antigens. *Immunity* **17**: 211–220.
- Boisgerault, F, Gross, DA, Ferrand, M, Poupiot, J, Darocha, S, Richard, I *et al.* (2013). Prolonged gene expression in muscle is achieved without active immune tolerance using microRNA 142.3p-regulated rAAV gene transfer. *Hum Gene Ther* **24**: 393–405.
- Akache, B, Grimm, D, Pandey, K, Yant, SR, Xu, H and Kay, MA (2006). The 37/67-kilodalton laminin receptor is a receptor for adeno-associated virus serotypes 8, 2, 3, and 9. *J Virol* **80**: 9831–9836.
- Walters, RW, Yi, SM, Keshavjee, S, Brown, KE, Welsh, MJ, Chiorini, JA *et al.* (2001). Binding of adeno-associated virus type 5 to 2,3-linked sialic acid is required for gene transfer. *J Biol Chem* **276**: 20610–20616.
- Hösel, M, Broxtermann, M, Janicki, H, Esser, K, Arzberger, S, Hartmann, P *et al.* (2012). Toll-like receptor 2-mediated innate immune response in human nonparenchymal liver cells toward adeno-associated viral vectors. *Hepatology* **55**: 287–297.
- Ponnazhagan, S, Mahendra, G, Curiel, DT and Shaw, DR (2001). Adeno-associated virus type 2-mediated transduction of human monocyte-derived dendritic cells: implications for ex vivo immunotherapy. *J Virol* **75**: 9493–9501.
- Veron, P, Allo, V, Rivière, C, Bernard, J, Douar, AM and Masurier, C (2007). Major subsets of human dendritic cells are efficiently transduced by self-complementary adeno-associated virus vectors 1 and 2. *J Virol* **81**: 5385–5394.
- Zhang, Y, Chirmule, N, Gao, GP and Wilson, J (2000). CD40 ligand-dependent activation of cytotoxic T lymphocytes by adeno-associated virus vectors *in vivo*: role of immature dendritic cells. *J Virol* **74**: 8003–8010.
- Lu, Y and Song, S (2009). Distinct immune responses to transgene products from rAAV1 and rAAV8 vectors. *Proc Natl Acad Sci USA* **106**: 17158–17162.
- Walczak, AP, Kramer, E, Hendriksen, PJ, Tromp, P, Helsen, JP, van der Zande, M, *et al.* (2014). Translocation of differently sized and charged polystyrene nanoparticles in *in vitro* intestinal cell models of increasing complexity. *Nanotoxicol* **1**–9.
- Rettig, L, Haen, SP, Bittermann, AG, von Boehmer, L, Curioni, A, Krämer, SD *et al.* (2010). Particle size and activation threshold: a new dimension of danger signaling. *Blood* **115**: 4533–4541.
- Seydoux, E, Rothen-Rutishauser, B, Nita, IM, Balog, S, Gazdhar, A, Stumbles, PA *et al.* (2014). Size-dependent accumulation of particles in lysosomes modulates dendritic cell function through impaired antigen degradation. *Int J Nanomedicine* **9**: 3885–3902.
- Kedmi, R, Ben-Arie, N and Peer, D (2010). The systemic toxicity of positively charged lipid nanoparticles and the role of Toll-like receptor 4 in immune activation. *Biomaterials* **31**: 6867–6875.
- Luonov, O, Syrovets, T, Loos, C, Nienhaus, GU, Mailänder, V, Landfester, K *et al.* (2011). Amino-functionalized polystyrene nanoparticles activate the NLRP3 inflammasome in human macrophages. *ACS Nano* **5**: 9648–9657.
- Keller, SA, Schwarz, K, Manolova, V, von Allmen, CE, Kinzler, MG, Bauer, M *et al.* (2010). Innate signaling regulates cross-priming at the level of DC licensing and not antigen presentation. *Eur J Immunol* **40**: 103–112.
- Faust, SM, Bell, P, Cutler, BJ, Ashley, SN, Zhu, Y, Rabinowitz, JE *et al.* (2013). CpG-depleted adeno-associated virus vectors evade immune detection. *J Clin Invest* **123**: 2994–3001.
- Zhu, J, Huang, X and Yang, Y (2009). The TLR9-MyD88 pathway is critical for adaptive immune responses to adeno-associated virus gene therapy vectors in mice. *J Clin Invest* **119**: 2388–2398.
- Girod, A, Wobus, CE, Zádori, Z, Ried, M, Leike, K, Tijssen, P *et al.* (2002). The VP1 capsid protein of adeno-associated virus type 2 is carrying a phospholipase A2 domain required for virus infectivity. *J Gen Virol* **83**(Pt 5): 973–978.
- Brazil, MI, Weiss, S and Stockinger, B (1997). Excessive degradation of intracellular protein in macrophages prevents presentation in the context of major histocompatibility complex class II molecules. *Eur J Immunol* **27**: 1506–1514.
- Varki, A (2009). Multiple changes in sialic acid biology during human evolution. *Glycoconj J* **26**: 231–245.
- Rivière, C, Danos, O and Douar, AM (2006). Long-term expression and repeated administration of AAV type 1, 2 and 5 vectors in skeletal muscle of immunocompetent adult mice. *Gene Ther* **13**: 1300–1308.
- Goyenvallé, A, Vulin, A, Fougerousse, F, Leturcq, F, Kaplan, JC, Garcia, L *et al.* (2004). Rescue of dystrophic muscle through U7 snRNA-mediated exon skipping. *Science* **306**: 1796–1799.
- Boisgerault, F, Rueda, P, Sun, CM, Hervas-Stubbs, S, Rojas, M and Leclerc, C (2005). Cross-priming of T cell responses by synthetic microspheres carrying a CD8+ T cell epitope requires an adjuvant signal. *J Immunol* **174**: 3432–3439.
- R Core Team (2015). R: a language and environment for statistical computing. R Foundation for Statistical Computing, Vienna, Austria. <http://www.R-project.org/>.
- Husson, F, Josse, J, Le, S and Mazet, J (2015). FactoMineR: multivariate exploratory data analysis and data mining. R package version 1.29. <http://CRAN.R-project.org/package=FactoMineR>.



This work is licensed under a Creative Commons Attribution-NonCommercial-NoDerivs 4.0 International License.

The images or other third party material in this article are included in the article's Creative Commons license, unless indicated otherwise in the credit line; if the material is not included under the Creative Commons license, users will need to obtain permission from the license holder to reproduce the material. To view a copy of this license, visit <http://creativecommons.org/licenses/by-nc-nd/4.0/>